Astronomical Data Analysis Software and Systems XV
ASP Conference Series, Vol. 351, 2006
C. Gabriel, C. Arviset, D. Ponz and E. Solano, eds.

X-ray Astronomy and the Analysis of X-ray Data

Jonathan C. McDowell
Smithsonian Astrophysical Observatory, 60 Garden St, Cambridge, MA 02138

Abstract. The Chandra X-ray Observatory, launched in 1999, continues to return spectacular scientific results thanks to its combination of high spatial and spectral resolution. I will discuss a selection of these results, and draw attention to the specific data analysis challenges posed by X-ray observatories in general, leading to the identification of the spatial distribution of elements in supernova remnants, the discovery of X-ray jets in galactic and extragalactic objects, the resolution of the X-ray background into faint sources, and the analysis of X-ray spectra of individual sources in external galaxies. The X-ray event list paradigm provides a compact representation of a sparse multidimensional dataset, supporting time- and energy-resolved hundred-megapixel images. In contrast to the case of HST and ground-based telescopes, the pointing of X-ray telescopes, while known accurately after the fact, is not kept constant during the observation. Sharp X-ray images are reconstructed from a dithered picture using star tracker data. The imaging point spread function and spectral energy response vary greatly across the field of view and must be carefully calibrated. For X-ray CCD data, the line spread function is broad and multi-peaked, driving us to forward-fitting solutions. For high resolution grating data, order separation is a challenge. Finally, in all X-ray data the low count rate and the ubiquitous cosmic X-ray background require careful statistical attention. Despite these complexities, the standard data analysis packages like CIAO, HEASOFT and SAS are mature enough to allow non-specialist users to reliably extract high quality science from X-ray observations.

1. Imaging Results from Chandra

We are now six years in to the missions of two great X-ray observatories - NASA's Chandra (Fig. 1), launched in July 1999, which has the highest spatial resolution, and ESA's XMM-Newton, launched in December 1999, which has the greatest collecting area. Both observatories feature imagers with intermediate spectral resolution and gratings with high spectral resolution; in this article I will concentrate on selected imaging results from Chandra's ACIS imager and the challenges these observations pose for software and data analysis.

A dramatic illustration of the power of high resolution spatial-spectral data is provided by the megasecond observation of the supernova remnant Cas A (Hwang et al 2004) (Fig. 2) in which the spatial distribution of the material is very different in silicon and iron line narrow-band images from its distribution in

Figure 1. The Chandra X-ray Observatory, launched into high Earth orbit in 1999

.

the continuum, revealing the presence of a silicon jet and clumps of iron ejecta inside the spherical shock. Time-resolved imaging of the Crab (Hester al al 2002) reveals X-ray features moving at 0.5c within the jet and torus discovered earlier with ROSAT. The ability of X-ray observatories to accumulate exposures over long periods of time bears fruit with deep surveys like the Chandra Deep Field North (Fig 3) (e.g. Brandt et al 2004, Alexander et al 2003). The CDFN accumulates 23 days of exposure time in 20 observations over a 3 year period, reaching a limiting sensitivity of two photons a week and resulting in a catalog of five hundred active galactic nuclei. The data analysis challenges include stacking with accurate relative and absolute astrometry; the Chandra calibration is usually good to 1 arcsecond across the field, but tweaking the solution can improve the registration further. The change in the spectral resolution and sensitivity of the instrument is significant over the period of observations, complicating spectral fits. The exposure map ('flat field') for each chip has discontinuous variations associated with the chip and node boundaries, and the point spread function (PSF) size is a strong function of distance from the field center, so the limiting sensitivity drops towards the edge of the field.

Observations of the super-merger galaxies NGC 6240 and Arp 220 involve careful data analysis both on small and large spatial scales. On the small scale, both galaxies may have binary supermassive black hole nuclei. For NGC 6240, Komossa et al (2003) were easily able to separate the two X-ray nuclei 1.5 arcsec apart. In contrast, the weaker evidence for X-ray detections at 0.5 arcsec separation of two nuclei in Arp 220 by Clements et al (2002) requires more agressive modelling with PSFs, and rebinning the data to sub-pixel resolution by taking advantage of the telescope dither. There are many contributions to uncertainties in the point spread function - mirror modelling, aspect reconstruction errors, and detector effects like charge transfer inefficiency, out-of-time events and bad pixels. These still limit our ability to study faint extent - like X-ray jets - near

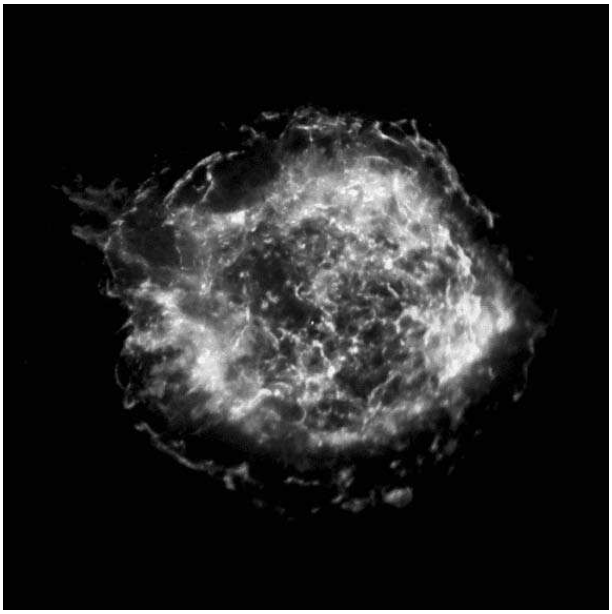

Figure 2. Three band image of Cas A showing silicon jet (Hwang et al 2003)

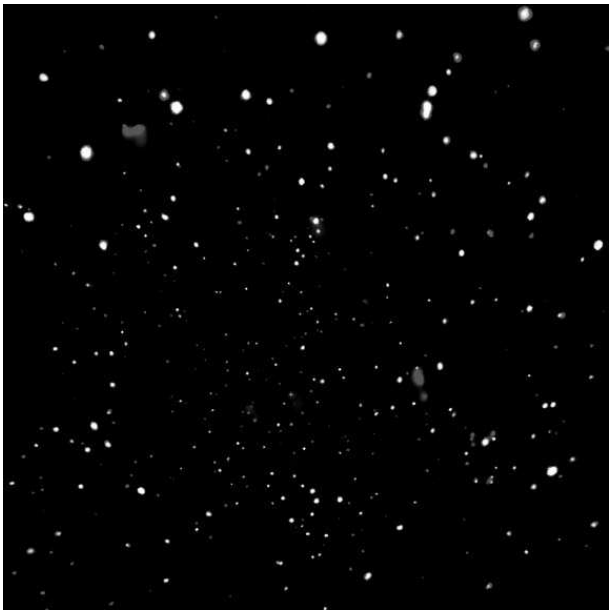

Figure 3. Hubble Deep Field North, showing increase in point spread function at large off-axis angles.

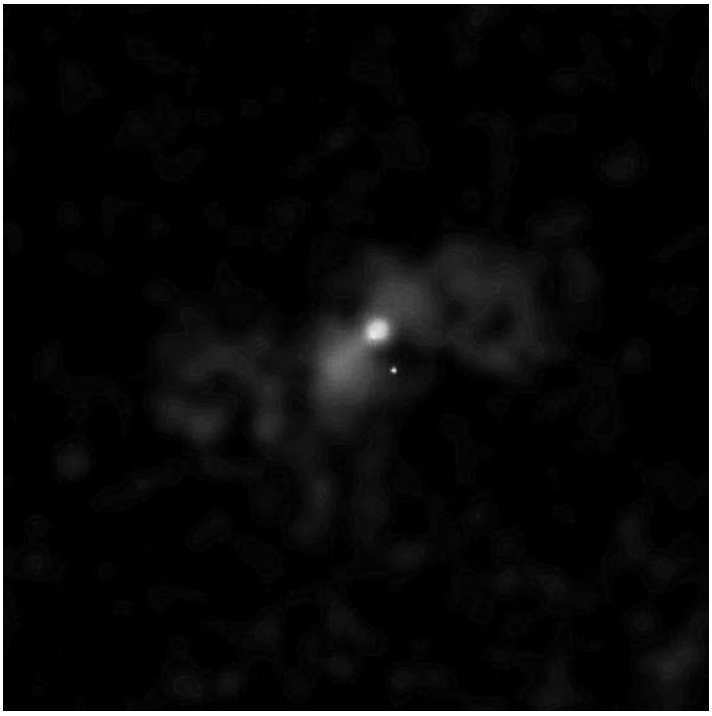

Figure 4. Arp 220

to bright sources in Chandra and other X-ray missions. On extended scales, the complex emission structures in Arp 220 (Fig. 4; McDowell et al 2003) are hard to pull out. To make the image seen here, we processed the data in three separate energy bands, subtracted the background; subtracted the brightest point soruces using a custom generated PSF, applied adaptive smoothing to the remaining data, added the PSFs back in, and recombined the bands into a true color image.

This procedure, as with most attempts to reconstruct X-ray images of extended sources, leaves you with a dataset which is not useful for measuring accurate fluxes. However, it does provide the observer with hypotheses that can be formally tested on the raw data, by isolating spatial regions of interest in the reconstructed image and re-extracting the corresponding photons from the original event list. For example, the shape of individual blobs making up the outer lobes of Arp 220 can't be trusted since each blob consists of only around 20 photons - the smoothing algorithm has amplified Poisson noise. But the fact that the outer lobes are annular is real, confirmed by tests on the total count rate in the lobe compared to that in the central hole. As always in the X-ray domain, we use fluxed, smoothed, deconvolved data to suggest a model, and then take a forward-folding approach - convolving the model with a telescope simulator and comparing with the data in raw count space - to validate or reject the model and fit its parameters.

2. X-ray Data Analysis

There are three main packages currently in wide use by X-ray astronomers: CIAO from the SAO/MIT Chandra team (`http://cxc.harvard.edu`), a general purpose analysis package optimized for spatial analysis and for Chandra; HEASOFT from Goddard (`http://heasarc.gsfc.nasa.gov`), a general purpose X-ray package; and SAS (`http://xmm.esac.esa.int`), a package specific to XMM-Newton data analysis. A ROSAT-era collaboration established common FITS standards for keywords and data file conventions, so that derived data products for all the missions are compatible with all the packages, permitting a great degree of interoperability.

Event lists The fundamental calibrated data product in X-ray astronomy is the 'event list', which includes a table in which each record represents an 'event' or possible detected photon, and each column represents some property of the photon detection such as position, energy, or an instrumental flag associated with the detection. By making a histogram of this table on one or more of the columns one makes derived products - an image by binning on a position column, a spectrum by binning on instrumental energy, a light curve by binning on event detection time. The event list also contains metadata describing the parameter space in which events could have been detected - notably the GTIs or 'good time intervals' giving times when events were not filtered out due to high background, sub-optimal detector configuration, bad pointing, etc. Most users first look at the event list with the ds9 (Joye and Mandel 2003) imager, which automatically locates the celestial coordinate columns and performs the 2-dimensional histogram to present the data in image form. While convenient, this often delays new X-ray users' understanding of the distinction between event-list and image data files; for X-ray analysis, it is important as you go back and forth between the event-list and image domains to understand which operations are meaningful on which data files. For example, once you have filtered the event list on energy and made an image in a particular band, that image no longer retains energy-resolved information.

Aspect solutions A second area of confusion is the fact that X-ray telescopes dither while observing, and reconstruct the image later using star tracker data. This is possible since the individual photons are time-tagged: we have a record of when a particular photon hit the detector and what its chip pixel coordinates were, and we also know what celestial position corresponded to that chip pixel at that instant. This approach is becoming somewhat familiar to Hubble observers who take multiple exposures with slightly different aimpoints and combine them after the fact; in the X-ray world each photon essentially corresponds to a single such exposure which must be offset, often by many arcseconds and possibly with a rotation, before being accumulated in a celestial coordinate image. Thus, the pixels in the celestial coordinate ('sky coordinate') image are not the instrument pixels - they are purely software pixels and may not even have the same size as the instrument pixels. This means that sky-plane calibrations and instrument-plane calibrations are matched to different coordinate systems and must be

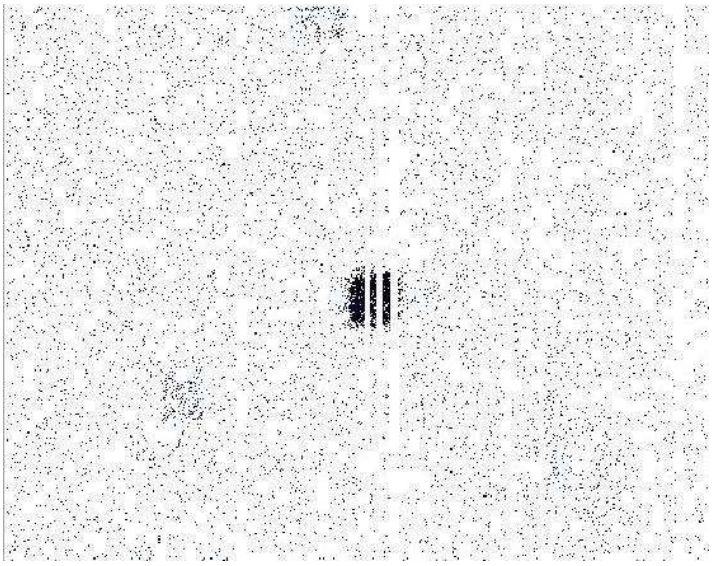

Figure 5. In instrument space the photons are spread out over many arcseconds and have bad detector columns going through them. The software is capable of correctly handling the change in effective exposure time. Most of the flux from this Chandra point source will fall in a single pixel after aspect reconstruction is applied; you could lose the source entirely if no dithering was applied and it landed on a bad pixel.

applied separately; a single pixel in the sky image maps to an average over many pixels on the detector (Fig. 5) and its calibration must be handled accordingly.

Exposure Maps Notwithstanding my remarks above about working in raw count space, it is sometimes useful to generate fluxed images. In X-ray astronomy usage, the term 'exposure map' usually refers to an image whose values are the flux-to-counts conversion factor, incorporating the effects of telescope vignetting, bad detector columns, inter-chip gaps, quantum efficiency spatial variations down to the pixel scale, and other geometric factors. (Note that the usage of 'exposure map' to refer to a map of effective exposure time, sometimes including only some of the above factors, is also found). Since the vignetting and QE effects are energy-dependent, an exposure map includes an assumption about the source spectra, and for careful work separate spectral fits to individual sources must be done (e.g. Davis 2001).

X-ray Spectral Calibration We may idealize the problem of observing an astronomical spectrum with a photon-counting detector as

$$N(E_p) = \int dE R(E, E_p) A(E) F(E).$$

Here E is the true photon energy, and E_p is the instrumentally measured photon energy (in X-ray astronomy, we use an integer-valued instrumental channel and

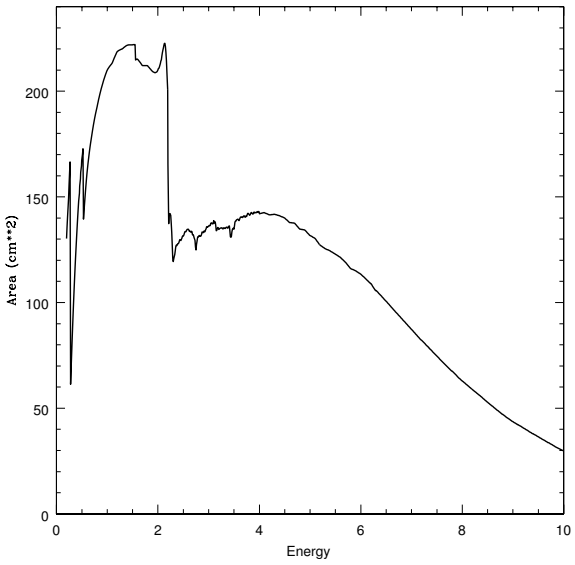

Figure 6. A plot of the energy transmission function A(E) for one of the Chandra-ACIS chips. Note the iridium edge near 2 keV due to the mirror coating.

call it the PHA value, an acronym originally referring to the electronics in a high voltage gas counter, but it's really no different from the wavelength bin in an optical spectrum). F(E) is the incident spectrum (including background; here I ignore detector background); A(E) is the instrument's geometric area multiplied by the energy-dependent transmission curve, and is called the 'effective area'. Its form is typically dominated by sharp atomic absorption edge features, see Fig. 6. $R(E, E_p)$ is the line spread function, referred to in X-ray astronomy as the redistribution matrix, and $N(E_p)$ is the observed count spectrum as a function of instrumental energy channel. In optical astronomy we usually ignore R in data analysis, set $E_p = E$, invert the equation to plot an approximate $F(E) = N(E)/A(E)$ and recall at the interpretation stage that the 'instrumental line width' contributes to the observed width of spectral features.

In X-ray astronomy the combination of low signal-to-noise and highly non-diagonal R (Fig. 7) has led to the tradition of rejecting this approximation; indeed deconvolution of the equation is usually not uniquely possible and instead we fit parameterized functions $F(E; q_i)$ to the data and evaluate a goodness-of-fit statistic in count space, with careful attention to the problems of binning in the low counts regime. The functions A and R are determined from the instrument calibration for the appropriate observation date, averaged over the detector region corresponding to the source photons, taking the telescope dither into account, and written to standard-format files called the ARF and the RMF. Together with the count spectrum, also in a standard format file called the PHA file, a variety of X-ray spectral fitting programs such as XSPEC (Arnaud 1996)

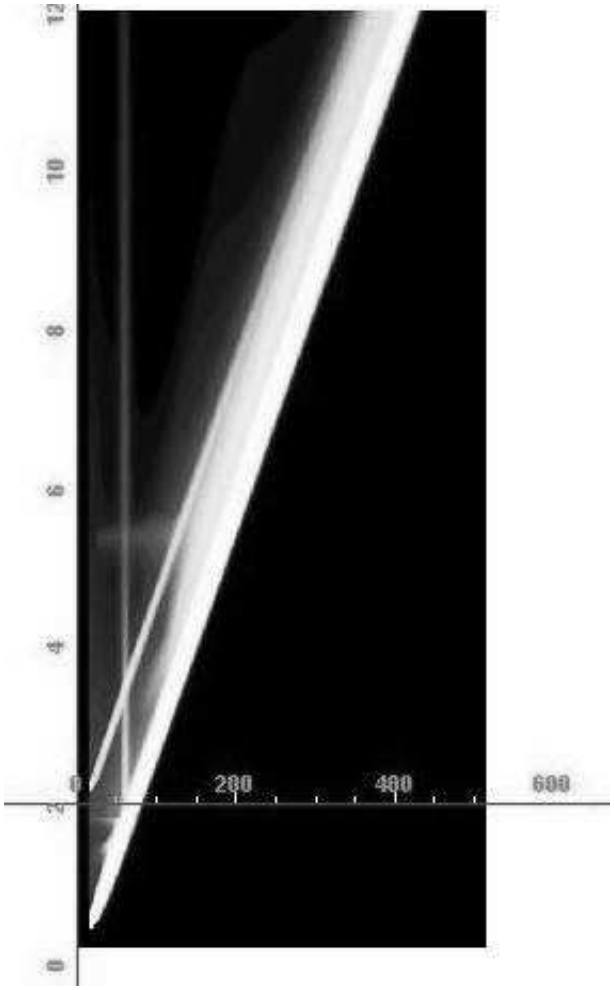

Figure 7. A plot of the line spread function $R(E, E_p)$, i.e. the probability that a photon of energy E will be detected as an event of energy E_p, for one of the Chandra-ACIS chips showing the complex off-diagonal structure. The X-axis is instrumental energy channel and the Y-axis is true photon energy in keV.

and Sherpa (Freeman, Doe and Siemiginowska 2001) can be used to analyse the spectra.

3. Summary

Science: Chandra and XMM-Newton have brought X-ray astronomy to a new level of sophistication, and it looks like it will be a long time before they are surpassed. Chandra's high resolution and XMM's large area each deliver unique science. The X-ray background has been resolved into active nuclei; spatial-spectral studies of supernova remnants have revealed the different histories of shocks, jets and ejecta; galaxy and cluster studies are providing a cosmic census of compact objects, revealing ultra-luminous X-ray sources, and elucidating the galacto-ecological role of the hot interstellar medium. High resolution imaging has shown that bright X-ray jets are common in quasars and that some merging galaxies have binary X-ray nuclei. The high resolution grating studies not discussed here provide understanding of the detailed atomic physics in the X-ray spectra of stars and extragalactic objects. Chandra data is available (typically after a one year proprietary period) from the archive at `http://cxc.harvard.edu/cda`, and an overview of the most photogenic results can be found at the press release site `http://chandra.harvard.edu`. The corresponding information for XMM-Newton is at `http://xmm.esac.esa.int` and access to all historic X-ray missions is provided at `http://heasarc.gsfc.nasa.gov`.

Data analysis: Remember –

- X-ray telescopes drift (dither) while observing, so the instrumental pixels are not the same as the sky (final image) pixels.
- When you publish a source with only three photons, make sure you understand the background. Correspondingly, when you read a paper about a feature in an X-ray source and only a flux is given, make sure to estimate how many counts they really have.
- The instrumental properties of X-ray telescopes tend to vary with off-axis angle, photon energy, and time.
- The tao of X-ray analysis: forward folding through a telescope simulator, followed by comparison with raw data, rather than fluxing and deconvolution.

Despite these complications, X-ray missions have high quality calibrated data in their archives, the software is freely available and interoperable, and we all use the same standardized data formats. The learning curve is therefore not too bad, and astronomers used to working in other wavebands shouldn't hesitate to apply for time on our observatories.

Acknowledgments. The author acknowledges support from the Chandra X-Ray Center, which is operated by the Smithsonian Astrophysical Observatory for and on behalf of NASA under contract NAS8-39073.

References

Alexander, D.M., et al 2003, AJ126, 539.

Arnaud, K.A., 1996, in ASP Conf. Ser., Vol. 101, ADASS V, ed. G. H. Jacoby & J. Barnes (San Francisco: ASP), p 17.

Brandt, W.N., et. al. 2004, in Frontiers of X-ray astronomy. (ed. Fabian, Pounds, Blandford), p 191.

Clements, D.L. et. al. 2002, ApJ581, 974.

Davis, J.E., 2001, ApJ548, 1010.

Freeman, P., Doe, S., and Siemiginowska, A., 2001, Proc. SPIE Vol 4477, p 76.

Hester, J., et. al. 2002, ApJ577, L49

Hwang, U., et. al., 2004, ApJ615, 117.

Joye, W.A. and Mandel, E., 2003, ADASS XII, ASP Conf. Vol. 295, p 489.

Komossa, S., et. al. 2003, ApJ582, L15.

McDowell. J.C., et al 2003, ApJ591, 154.